

A conformal mapping method in inverse obstacle scattering

Houssem Haddar, Rainer Kress

► **To cite this version:**

Houssem Haddar, Rainer Kress. A conformal mapping method in inverse obstacle scattering. Complex Variables and Elliptic Equations, Taylor

Francis, 2013. <hal-00768726>

HAL Id: hal-00768726

<https://hal.inria.fr/hal-00768726>

Submitted on 23 Dec 2012

HAL is a multi-disciplinary open access archive for the deposit and dissemination of scientific research documents, whether they are published or not. The documents may come from teaching and research institutions in France or abroad, or from public or private research centers.

L'archive ouverte pluridisciplinaire **HAL**, est destinée au dépôt et à la diffusion de documents scientifiques de niveau recherche, publiés ou non, émanant des établissements d'enseignement et de recherche français ou étrangers, des laboratoires publics ou privés.

A conformal mapping method in inverse obstacle scattering

Housseem Haddar* and Rainer Kress†

November 7, 2012

Abstract

Akduman, Haddar and Kress [1, 5, 11] have employed a conformal mapping technique for the inverse problem to reconstruct a perfectly conducting inclusion in a homogeneous background medium from Cauchy data for electrostatic imaging, that is, for solving an inverse boundary value problem for the Laplace equation. We propose an extension of this approach to inverse obstacle scattering for time-harmonic waves, that is, to the solution of an inverse boundary value problem for the Helmholtz equation. The main idea is to use the conformal mapping algorithm in an iterative procedure to obtain Cauchy data for a Laplace problem from the given Cauchy data for the Helmholtz problem. We present the foundations of the method together with a convergence result and exhibit the feasibility of the method via numerical examples.

1 Introduction

The mathematical modeling of the use of electrostatic (or magnetostatic) methods or electromagnetic wave scattering methods in various non-destructive testing and evaluation schemes leads to a variety of inverse boundary value problems for the Laplace and the Helmholtz equation. In principle, in the corresponding two-dimensional model problems, in many of these applications an unknown inclusion

*Ecole Polytechnique, Route de Saclay, 91128 Palaiseau Cedex, France (haddar@cmapx.polytechnique.fr)

†University of Göttingen, Lotzestrasse 16-18 D-37083 Göttingen, Germany (kress@math.uni-goettingen.de)

within a homogeneous conducting host medium is assessed from over determined Cauchy data on an accessible closed curve surrounding the unknown object.

For simplicity of our presentation, we assume that D_0 and D_1 are two simply connected bounded domains in \mathbb{R}^2 with C^1 smooth boundaries $\Gamma_0 := \partial D_0$ and $\Gamma_1 := \partial D_1$ such that $\overline{D_0} \subset D_1$ and denote by D the doubly connected domain $D := D_1 \setminus \overline{D_0}$. The inverse problems we are concerned with is to determine the unknown interior boundary curve Γ_0 from the Cauchy data

$$f := u|_{\Gamma_1} \quad \text{and} \quad g := \frac{\partial u}{\partial \nu}|_{\Gamma_1} \quad (1.1)$$

on Γ_1 of a solution $u \in H^1(D)$ of the Laplace equation $\Delta u = 0$ or the Helmholtz equation $\Delta u + k^2 u = 0$ with wave number $k > 0$ satisfying the homogeneous Dirichlet condition

$$u = 0 \quad (1.2)$$

on Γ_0 . Here, the unit normal ν to Γ_1 is assumed to be directed into the exterior of D_1 .

For the Laplace case over the last decade Akduman, Haddar and Kress [1, 5, 6, 7, 11, 12] have developed and analyzed an inverse algorithm for the above inverse Dirichlet problem together with extensions to other boundary conditions. To describe the main idea of this approach, in the sequel we will identify \mathbb{R}^2 and \mathbb{C} in the usual manner. We introduce the annulus B bounded by two concentric circles C_0 with radius $\rho < 1$ and C_1 with radius one centered at the origin. By the Riemann conformal mapping theorem for doubly connected domains (see [15]) there exists a uniquely determined radius ρ and a holomorphic function Ψ that maps B bijectively onto D such that the boundaries C_0 and C_1 are mapped onto Γ_0 and Γ_1 , respectively, with all boundary curves in counter clockwise orientation. The function Ψ is unique up to a rotation of the annulus B . We parameterize the exterior boundary

$$\Gamma_0 = \{\gamma(t) : t \in [0, 2\pi)\}$$

by a continuously differentiable 2π periodic function $\gamma : \mathbb{R} \rightarrow \mathbb{C}$ with the property that $\gamma|_{[0, 2\pi)}$ is injective. The latter, in particular, implies that $|\gamma'(t)| \neq 0$ for all $t \in [0, 2\pi]$. We fix the freedom in rotating B by prescribing $\Psi(1) = \gamma(0)$ and define a boundary correspondence function $\varphi : [0, 2\pi] \rightarrow [0, 2\pi]$ by setting

$$\varphi(t) := \gamma^{-1}(\Psi(e^{it})), \quad t \in [0, 2\pi]. \quad (1.3)$$

Clearly, the boundary values φ uniquely determine Ψ as the solution to the Cauchy problem with $\Psi|_{C_1}$ given by $\Psi(e^{it}) = \gamma(\varphi(t))$ for $t \in [0, 2\pi]$.

The main ingredient of the conformal mapping method for the solution of the inverse Dirichlet problem for the Laplace equation is an ordinary differential equation for the boundary correspondence function φ . We denote by $A_\rho : H^{1/2}[0, 2\pi] \rightarrow H^{-1/2}[0, 2\pi]$ the Dirichlet-to-Neumann operator for the annulus B that maps functions $\tilde{f} \in H^{1/2}[0, 2\pi]$ onto the normal derivative

$$\left(A_\rho \tilde{f}\right)(t) := \frac{\partial v}{\partial \nu}(e^{it}), \quad t \in [0, 2\pi], \quad (1.4)$$

of the harmonic function $v \in H^1(B)$ with boundary values on C_1 and C_0 given by

$$v(e^{it}) = \tilde{f}(t) \quad \text{and} \quad v(\rho e^{it}) = 0 \quad \text{for } t \in [0, 2\pi].$$

Via $v := u \circ \Psi$ we associate the harmonic function u in D with a harmonic function v in B and can use the Cauchy–Riemann equations for u and v and their harmonic conjugates to derive the nonlocal differential equation

$$\varphi' = \frac{A_\rho(f \circ \gamma \circ \varphi)}{|\gamma' \circ \varphi| g \circ \gamma \circ \varphi} \quad (1.5)$$

together with the boundary conditions

$$\varphi(0) = 0, \quad \varphi(2\pi) = 2\pi \quad (1.6)$$

for the boundary correspondence function φ as the central piece of the inverse algorithm. Note, that (1.5) is slightly more general than in [1, 5, 11] since here we do not assume that Γ_1 is parameterized by arc length. The differential equation has to be complemented by an equation for the radius ρ obtained by applying Green’s integral theorem to v and an appropriate harmonic test function w in B . Its simplest version

$$\rho = \exp\left(-\frac{\int_0^{2\pi} f \circ \gamma \circ \varphi dt}{\int_{\Gamma_1} g ds}\right) \quad (1.7)$$

is obtained by choosing $w(x) = \ln|x|$. However, eventually we want to employ the algorithm to the restriction of bounded harmonic functions $u \in H_{\text{loc}}^1(\mathbb{R}^2 \setminus \bar{D}_0)$ and in this case equation (1.7) fails because here the normal derivative g has mean value zero over Γ_0 (see [10]). Hence we rely on the quadratic equations

$$[|m| a_m(\varphi; f) + b_m(\varphi; g)] \rho^{2|m|} + |m| a_m(\varphi; f) - b_m(\varphi; g) = 0, \quad m \neq 0, \quad (1.8)$$

in terms of the Fourier coefficients

$$a_m(\varphi; f) := \int_0^{2\pi} f(\gamma(\varphi(t))) e^{-imt} dt, \quad b_m(\varphi; g) := \int_0^{2\pi} g(\gamma(\varphi(t))) \varphi'(t) e^{-imt} dt,$$

which is obtained using $w(x) = r^m e^{\pm im\theta}$ (in polar coordinates (r, θ) for x) as test function. From this we observe that if $|m|a_m \neq 0$ then $b_m \pm |m|a_m \neq 0$ and we can solve (1.8) to obtain

$$\rho = c_m(\varphi; f, g) \quad (1.9)$$

where we have set

$$c_m(\varphi; f, g) := \left[\frac{b_m(\varphi; g) - |m|a_m(\varphi; f)}{b_m(\varphi; g) + |m|a_m(\varphi; f)} \right]^{\frac{1}{2|m|}}. \quad (1.10)$$

Under appropriate assumptions it can be shown that (1.5) and (1.9) can be solved by successive approximations [1, 5]. Once φ and ρ are available the highly ill-posed Cauchy problem to determine the holomorphic functions Ψ in B from its boundary values φ can be solved by a Laurent expansion that need to be stabilized, for example, by a Tikhonov type regularization.

In accordance with the uniqueness for the above inverse Dirichlet problem for the Laplace equation, in principle one pair of real valued Cauchy data suffices for the conformal mapping algorithm to work. However, to cope with the difficulty arising from possible zeros of g a variant of the algorithm using two pairs of real valued Cauchy data has been developed in [5]. In the application to inverse scattering problems further below we always will have complex valued Cauchy data, that is, two pairs of real valued Cauchy data. In this case, the differential equation to be used has the form

$$\frac{d\varphi}{dt} = \frac{\Re[(\bar{g} \circ \gamma \circ \varphi) A_\rho(f \circ \gamma \circ \varphi)]}{|\gamma' \circ \varphi| |g \circ \gamma \circ \varphi|^2} \quad (1.11)$$

which is obtained as a combination of (1.5) for the real and imaginary parts of the Cauchy data.

Summarizing, the conformal mapping method for the Laplace case defines a solution operator R taking the Cauchy data f, g onto the interior boundary curve Γ_0 , that is,

$$\Gamma_0 = R(f, g). \quad (1.12)$$

Its regularized version R_α with regularization parameter $\alpha > 0$ leads to the regularized solution

$$\Gamma_{0,\alpha} = R_\alpha(f, g). \quad (1.13)$$

The setting in the development of the conformal mapping method in [1, 5, 11] always has been a Dirichlet boundary value problem for a solution $u \in H^1(D)$ for the Laplace equation in the doubly connected domain D with boundary conditions $u = 0$ on Γ_0 and $u = f$ on Γ_1 for a given $f \in H^{1/2}(\Gamma_1)$ with the goal to reconstruct

the unknown Γ_0 from f and the resulting normal derivative $g \in H^{-1/2}(\Gamma_1)$. The most natural extension to the Helmholtz equation would treat the corresponding inverse problem for solutions $u \in H^1(D)$ to the Helmholtz equation in D . However, we have chosen to slightly modify the setting and consider inverse scattering problems in an exterior domain, although we note that the following analysis, in principle, also covers the inverse problem for the Helmholtz equation in the bounded domain D .

Given incident fields $u_{i,0}$ and $u_{i,k}$ by solutions to the Laplace and Helmholtz equation in D_1 respectively, we now consider the scattering problems for solutions u_0, u_k in $H_{\text{loc}}^1(\mathbb{R}^2 \setminus \bar{D}_0)$ to the Laplace equation $\Delta u_0 = 0$ or the Helmholtz equation $\Delta u_k + k^2 u_k = 0$ in $\mathbb{R}^2 \setminus \bar{D}_0$ satisfying the Dirichlet boundary conditions

$$u_0 = -u_{i,0} \quad \text{and} \quad u_k = -u_{i,k} \quad \text{on } \Gamma_0 \quad (1.14)$$

together with an appropriate condition at infinity. In particular, for the Helmholtz case we require the Sommerfeld radiation condition (see [2, 10]) for the scattered field u_k . If for the Laplace case we assume boundedness for u_0 then from the low wave number estimates for the difference of solutions to exterior boundary value problems for the Helmholtz and Laplace equation due to Kress [8] and Werner [16] we only have a slow convergence $u_k \rightarrow u_0$ of order $1/|\ln k|$ as $k \rightarrow 0$. Hence, in order to improve on the speed of convergence we require that

$$u_0(x) = a \ln \frac{1}{|x|} + v_0(x), \quad x \in \mathbb{R}^2 \setminus \bar{D}_0, \quad (1.15)$$

where v_0 is bounded at infinity and the choice of the constant a will be specified later. Here, without loss of generality we assume that the origin is contained in D_0 .

The solutions of the two exterior Dirichlet problems define operators F_0 and F_k that for fixed incident fields $u_{i,0}$ and $u_{i,k}$ map the interior boundary Γ_0 onto the Cauchy data (f_L, g_L) and (f_H, g_H) of the total fields $u_0^{\text{tot}} := u_0 + u_{i,0}$ and $u_k^{\text{tot}} := u_k + u_{i,k}$ on Γ_1 , respectively, that is, the Cauchy data on Γ_1 are given by

$$(f_L, g_L) = F_0(\Gamma_0) \quad \text{and} \quad (f_H, g_H) = F_k(\Gamma_0).$$

Combining both equations and inserting (1.12) for Γ_0 yields

$$(f_L, g_L) = (f_H, g_H) + F_0(R(f_L, g_L)) - F_k(R(f_L, g_L)), \quad (1.16)$$

which, given the Cauchy data (f_H, g_H) for the Helmholtz solution u_k^{tot} , can be interpreted as a fixed point equation for the Cauchy data (f_L, g_L) for the Laplace solution u_0^{tot} . We may try solving it via successive approximations

$$(f_{n+1}, g_{n+1}) := (f_H, g_H) + F_0(R(f_n, g_n)) - F_k(R(f_n, g_n)), \quad n = 0, 1, \dots, \quad (1.17)$$

starting with the given Helmholtz data as initial guess $(f_0, g_0) = (f_H, g_H)$ and use the regularized version R_α of the solution operator. Each iteration step consists of two parts. First the conformal mapping algorithm for the Laplace case is applied with Cauchy data (f_n, g_n) to obtain an approximation Γ_n for the interior boundary curve. Then in the second part both boundary value problems (1.14) are solved for the interior boundary Γ_n to obtain $F_0(R(f_n, g_n))$ and $F_k(R(f_n, g_n))$ in order to update the Cauchy data via (1.17).

The purpose of this research is to establish a local convergence result for the iteration scheme (1.17) for small wave numbers and exhibit the feasibility of the proposed algorithm through some numerical examples. The plan of the paper is as follows: In Section 2 we will analyze the solution operator R occurring in (1.17) more closely and establish a Lipschitz condition for the regularized solution operator R_α . This is followed in Section 3 by the preparation of the low wave number estimates for the difference $F_k - F_0$ that are required in the convergence analysis of the iteration scheme which is the topic of the following Section 4. The final Section 5 is devoted to a short description of the numerical implementation and some numerical examples.

In principle, our algorithm belongs to the general class of methods in inverse obstacle scattering that create a sequence of boundary curves Γ_n by solving the forward problem for Γ_n and use this solution to update Γ_n into Γ_{n+1} , for example in the various types of regularized Newton iterations that have been developed in the literature, see [3] among many others. The new features in the conformal mapping algorithm are two-fold. Firstly, as counterpart to the many low wave number iterative procedures to solving the direct scattering problem (see [4]) it provides a first algorithm of this type for the inverse scattering problem. Secondly, a rare convergence result for the method was attainable. We note that in a similar iterative manner in [13] the solution of an inverse source problem for the Helmholtz equation is reduced to the solution of a corresponding inverse source problem for the Laplace equation.

2 The conformal mapping operator

The solution operator R given by the conformal mapping method consists of two parts. In the first part we solve the nonlocal differential equation (1.11) with boundary condition (1.6) for the boundary correspondence map φ by a fixed point equation for the operator

$$T(\psi; f, g)(t) := \int_0^t \left[U(\psi; f, g)(\tau) - \frac{1}{2\pi} \int_0^{2\pi} U(\psi; f, g)(\theta) d\theta \right] d\tau, \quad t \in [0, 2\pi], \quad (2.1)$$

where

$$U(\psi; f, g) := \frac{\Re [(\bar{g} \circ \gamma \circ V\psi) A_{c_m(V\psi; f, g)}(f \circ \gamma \circ V\psi)]}{|\gamma' \circ V\psi| |g \circ \gamma \circ V\psi|^2}$$

and

$$(V\psi)(t) := t + \psi(t), \quad t \in [0, 2\pi].$$

Let $X = H_0^1[0, 2\pi]$ and $Y = H^{1/2}(\Gamma_1) \times H^{-1/2}(\Gamma_1)$ and, for the remainder of the paper, assume that the requirements of Theorem 3.1 and Corollary 3.2 in [5] are satisfied, that is, D does not differ too much from the annulus B and the Cauchy data (f_L, g_L) for the Laplace problem are such that for some $m \neq 0$ there exists a closed ball $B_Y := B[f_L, g_L; r] \subset Y$ centered at (f_L, g_L) with radius r and a closed ball $B_X := B[0; p] \subset H_0^1[0, 2\pi]$ centered at $\psi_0 = 0$ with radius p such that $T : B_X \rightarrow B_X$ is a contraction operator for all pairs $(f, g) \in B_Y$, that is, the fixed point iterations

$$\psi_{n+1} := T(\psi_n; f, g), \quad n = 0, 1, 2, \dots, \quad (2.2)$$

starting with $\psi_0 = 0$ converge for any pair $(f, g) \in B_Y$ to some $\psi = \psi(f, g)$ in $H_0^1[0, 2\pi]$ representing the solution $\varphi = V\psi$ of (1.11) and (1.6). Simultaneously also the radius ρ is known through (1.9) and bounded away from zero and one. In the sequel we will refer to the above as **Assumption I**.

On $V := B_X \times B_Y \subset X \times Y$ we define the operator

$$G(\psi; f, g) := \psi - T(\psi; f, g).$$

Then G has partial Fréchet derivatives in V with respect to all variables and these derivatives are continuous. For the explicit form of the derivative with respect to ψ we refer to [5] and the derivatives with respect to f and g are similar in structure. In particular, inspecting the form of the derivatives, we can assume that V is chosen such that all three derivatives are uniformly bounded on V . By our assumptions the Fréchet derivative

$$\partial G(\psi_0; f_L, g_L) = I - \partial_\psi T(\psi_0; f_L, g_L),$$

where ψ_0 is the limit of the fixed point iterations (2.2) for the Laplace data pair (f_L, g_L) has a bounded inverse, since $\partial_\psi T(\psi_0; f_L, g_L)$ has spectral radius less than one by Theorem 3.1 in [5]. Because of $G(\psi_0; f_L, g_L) = 0$, from the implicit function theorem, we can conclude that the ball B_Y can be assumed to be chosen such that there exists a unique mapping $H : B_Y \rightarrow X$ with the properties

$$G(H(f, g); f, g) = 0, \quad (f, g) \in B_Y,$$

and $H(f_L, g_L) = \psi_0$. Furthermore, by the implicit function theorem, H is Fréchet differentiable with

$$\begin{aligned}\partial_f H(f, g) &= -[\partial_\psi G(\psi; f, g)]^{-1} \partial_f G(\psi; f, g), \\ \partial_g H(f, g) &= -[\partial_\psi G(\psi; f, g)]^{-1} \partial_g G(\psi; f, g).\end{aligned}\tag{2.3}$$

In particular, with the aid of the mean value theorem we can estimate

$$\|H(f_1, g_1) - H(f_2, g_2)\|_X \leq c \|(f_1, g_1) - (f_2, g_2)\|_Y\tag{2.4}$$

for all $(f_1, g_1), (f_2, g_2) \in B_Y$ and some constant c .

Clearly, we have that

$$R_\alpha = P_\alpha \circ H\tag{2.5}$$

in terms of the regularized solution operator P_α for the Cauchy problem. The linear operator $P_\alpha : \varphi = V\psi \rightarrow \Psi_\alpha|_{C_0}$ mapping the boundary correspondence function φ to the restriction of the regularized solution Ψ_α of the Cauchy problem is bounded, for example, with respect to the C^1 norm on the image space. Since a Tikhonov regularization is involved in Ψ_α its norm can be estimated by

$$\|\Psi_\alpha\|_{H_0^1[0, 2\pi] \rightarrow C^1[0, 2\pi]} \leq \frac{\beta}{\sqrt{\alpha}}\tag{2.6}$$

for some constant β (see [10]). Combining (2.4) and (2.6) we obtain the following lemma.

Lemma 2.1 *Under the Assumption I the regularized solution operator R_α of the conformal mapping method satisfies a Lipschitz condition*

$$\|R_\alpha(f_1, g_2) - R_\alpha(f_2, g_2)\|_{C^1[0, 2\pi]} \leq \frac{C}{\sqrt{\alpha}} \|(f_1, g_1) - (f_2, g_2)\|_{H^{1/2}(\Gamma_1) \times H^{-1/2}(\Gamma_1)}\tag{2.7}$$

for all $(f_1, g_1), (f_2, g_2) \in B_Y$ and some constant C .

This concludes our investigation of the solution operator R as part of the iteration operator in (1.17).

3 The boundary to Cauchy data operators

We now proceed with analyzing the difference between the boundary to Cauchy data operators F_0 and F_k for the Laplace and Helmholtz problems. In order to prove a contraction property of the iteration operator

$$J_\alpha(f, g) := (f_H, g_H) + (F_0 - F_k)(R_\alpha(f, g)),\tag{3.1}$$

for the regularized version of (1.17) via the mean value theorem we need a low wave number estimate for the difference of the Fréchet derivative $F'_0(\Gamma) - F'_k(\Gamma)$ for all boundary curves Γ in a neighborhood of Γ_0 . For this we consider the set of curves

$$W_\eta := \{\Gamma_{0,h} := \{x + h(x) : x \in \Gamma_0\} : h \in C^1(\Gamma_0), \|h\|_{C^1} \leq \eta\} \quad (3.2)$$

where $\eta > 0$ is chosen such that all $\Gamma_{0,h} \in W_\eta$ are boundaries of simply connected domains $D_{0,h}$ with $\bar{D}_{0,h} \subset D_1$.

In terms of the fundamental solutions

$$\Phi_0(x, y) := \frac{1}{2\pi} \ln \frac{1}{|x - y|}$$

to the Laplace equation and

$$\Phi_k(x, y) := \frac{i}{4} H_0^{(1)}(k|x - y|)$$

to the Helmholtz equation, for $\kappa = 0$ and $\kappa = k$ we define single-layer operators $\mathcal{S}_\kappa : H^{-1/2}(\Gamma_0) \rightarrow H_{\text{loc}}^1(\mathbb{R}^2 \setminus \bar{D}_0)$ by

$$(\mathcal{S}_\kappa \chi)(x) := \int_{\Gamma_0} \Phi_\kappa(x, y) \chi(y) ds(y), \quad x \in \mathbb{R}^2 \setminus \bar{D}_0, \quad (3.3)$$

and single-layer boundary integral operators $S_\kappa : H^{-1/2}(\Gamma_0) \rightarrow H^{1/2}(\Gamma_0)$ by the trace

$$S_\kappa \chi := (\mathcal{S}_\kappa \chi)|_{\Gamma_0}$$

on Γ_0 . Further, for notational convenience we introduce the mean values $\mathcal{M} : H^{-1/2}(\Gamma_0) \rightarrow H_{\text{loc}}^1(\mathbb{R}^2 \setminus \bar{D}_0)$ and $M : H^{-1/2}(\Gamma_0) \rightarrow H^{1/2}(\Gamma_0)$ by

$$(\mathcal{M}\chi)(x) := \frac{1}{|\Gamma_0|} \int_{\Gamma_0} \chi(y) ds(y), \quad x \in \mathbb{R}^2 \setminus \bar{D}_0,$$

and $M\chi := (\mathcal{M}\chi)|_{\Gamma_0}$. Here, by $|\Gamma_0|$ we denote the length of Γ_0 . We define $\mathcal{L}_k, \mathcal{L}_0 : H^{-1/2}(\Gamma_0) \rightarrow H_{\text{loc}}^1(\mathbb{R}^2 \setminus \bar{D}_0)$ by

$$\mathcal{L}_k := \left(1 - \frac{2\pi}{\ln k}\right) \mathcal{S}_k - \mathcal{S}_k M \quad (3.4)$$

and

$$\mathcal{L}_0 := \left(1 - \frac{2\pi}{\ln k}\right) \mathcal{S}_0 - \mathcal{S}_0 M + \beta_k \mathcal{M} \quad (3.5)$$

where

$$\beta_k = \frac{1}{\ln k} \left(\ln \frac{k}{2} - \frac{i\pi}{2} + C \right)$$

and C denotes Euler's constant. Finally, for $\kappa = k$ and $\kappa = 0$ we introduce $L_\kappa : H^{-1/2}(\Gamma_0) \rightarrow H^{1/2}(\Gamma_0)$ by $L_\kappa \chi := (\mathcal{L}_\kappa \chi)|_{\Gamma_0}$. We note that for the Laplace case $\kappa = 0$ the operators \mathcal{L}_0 and L_0 depend on the wavenumber k through the constant β_k . For simplicity of notation we refrained from indicating this by writing $\mathcal{L}_{0,k}$ and $L_{0,k}$ instead of \mathcal{L}_0 and L_0 . In particular, \mathcal{L}_0 and L_0 are not the limits of \mathcal{L}_k and L_k as $k \rightarrow 0$.

Motivated by the analysis in [8, 9], both for $\kappa = k$ and $\kappa = 0$, we seek the solution to the exterior Dirichlet problem (1.14) in the form of a single-layer potential

$$u_\kappa \chi_\kappa = \mathcal{L}_\kappa \chi_\kappa \quad (3.6)$$

with density $\chi_\kappa \in H^{-1/2}(\Gamma_0)$. Clearly, u_k satisfies the Sommerfeld radiation condition and u_0 is of the form (1.15) with

$$a = -\frac{1}{\ln k} \int_{\Gamma_0} \chi_0 ds. \quad (3.7)$$

For both $\kappa = k$ and $\kappa = 0$ the boundary condition (1.14) is satisfied provided the density χ_κ satisfy the integral equation

$$L_\kappa \chi_\kappa = -u_{i,\kappa}|_{\Gamma_0}. \quad (3.8)$$

Clearly, the definition of the integral operators and the integral equation (3.8) extend to all curves $\Gamma \in W_\eta$.

The operator $L : H^{-1/2}(\Gamma_0) \rightarrow H^{1/2}(\Gamma_0)$ given by

$$L = S_0 - S_0 M + M$$

is an isomorphism, see for example [10]. Therefore, in view of

$$L - L_0 = (1 - \beta_k)M + \frac{2\pi}{\ln k} S_0$$

a Neumann series argument implies that L_0 is an isomorphism, provided k is sufficiently small.

From the proof of Theorem 6.20 in [10] we have the existence of a function $\alpha \in H^{-1/2}(\Gamma_0)$ satisfying $S_0 \alpha = 1$ and $\xi := M \alpha \neq 1$. Taking the L^2 inner product of the integral equation (3.8) for $\kappa = 0$ with α and using the self-adjointness of S_0 we obtain that

$$\frac{b_k}{\ln k} \int_{\Gamma_0} \chi_0 ds = \int_{\Gamma_0} \alpha u_{i,0} ds \quad (3.9)$$

where

$$b_k := 2\pi - \xi \left(\ln \frac{k}{2} - \frac{i\pi}{2} + C \right).$$

For sufficiently small k we have $\beta_k \neq 0$ and therefore inserting (3.9) into (3.7) finally the coefficient for u_0 in the decomposition (1.15) can be specified as

$$a = a_k = -\frac{1}{b_k} \int_{\Gamma_0} \alpha u_{i,0} ds. \quad (3.10)$$

In the sequel by c we denote a generic constant that differs for each inequality. From the asymptotic behavior of the Hankel function $H_0^{(1)}(t)$ as $t \rightarrow 0$ it can be seen that

$$\|(L_k - L_0)\chi\|_{H^{1/2}(\Gamma)} \leq c |\ln k| k^2 \|\chi\|_{H^{-1/2}(\Gamma)} \quad (3.11)$$

for all $\Gamma \in W_\eta$ and all $\chi \in H^{-1/2}(\Gamma)$. Furthermore the operators L_0 are uniformly bounded for all $\Gamma \in W_\eta$. Then again a Neumann series argument shows that for all sufficiently small k the operator L_k is an isomorphism and for the unique solutions of the integral equations (3.8) we have

$$\|\chi_k - \chi_0\|_{H^{-1/2}(\Gamma)} \leq c (|\ln k| k^2 \|u_{i,0}\|_{H^{1/2}(\Gamma)} + \|u_{i,k} - u_{i,0}\|_{H^{1/2}(\Gamma)}) \quad (3.12)$$

for all $\Gamma \in W_\eta$. Analogously to (3.11) for the traces on Γ_1 we have that

$$\|(\mathcal{L}_k - \mathcal{L}_0)\chi\|_{H^{1/2}(\Gamma_1)} \leq c |\ln k| k^2 \|\chi\|_{H^{-1/2}(\Gamma)} \quad (3.13)$$

and the same order estimate also holds for the normal derivative of $\|(\mathcal{L}_k - \mathcal{L}_0)\chi$ on Γ_1 . Combining this with (3.12) and using the triangle inequality we obtain that

$$\|F_k(\Gamma) - F_0(\Gamma)\|_Y \leq c (|\ln k| k^2 \|u_{i,0}\|_{H^1(D_1)} + \|u_{i,k} - u_{i,0}\|_{H^1(D_1)}) \quad (3.14)$$

for all $\Gamma \in W_\eta$. Here, on the right hand side we have combined the $H^{1/2}$ norm over Γ arising from the insertion of (3.12) in the difference of the scattered fields and the $H^{1/2}$ norm over Γ_1 coming from the difference of the incident fields via the trace theorem into the H^1 norm over the domain D_1 .

For the Fréchet derivative of F_0 and F_k with respect to the boundary Γ_0 we first need to investigate the Fréchet differentiability of the solution to the integral equations (3.8). To this end, the boundary integral operators have to be transformed onto a fixed integration domain via parameterization

$$\{\Gamma_0 : x = z(t), 0 \leq t < 2\pi\}$$

in terms of a regular 2π periodic C^1 parameterization z of Γ_0 . The parameterized single-layer operator $\tilde{S}_\kappa : H^{-1/2}[0, 2\pi] \rightarrow H^{1/2}[0, 2\pi]$ defined by

$$\tilde{S}_\kappa(|z'| \chi \circ z) = (S_\kappa \chi) \circ z$$

for all $\chi \in H^{-1/2}(\Gamma_0)$ has the form

$$(\tilde{S}_\kappa \varphi)(t) = \int_0^{2\pi} \Phi_\kappa(z(t), z(\tau)) \varphi(\tau) d\tau, \quad t \in [0, 2\pi].$$

Its Fréchet derivative $\tilde{S}'_\kappa(\cdot; z, \zeta)$ at z in direction $\zeta \in C^1[0, 2\pi]$ is obtained by taking the Fréchet derivative of the kernel [14], that is, it is given by

$$\tilde{S}'_\kappa(\varphi; z, \zeta)(t) = \int_0^{2\pi} \text{grad}_x \Phi_\kappa(z(t), z(\tau)) \cdot \{\zeta(t) - \zeta(\tau)\} \varphi(\tau) d\tau, \quad t \in [0, 2\pi].$$

The asymptotics of the Hankel function $H_1^{(1)}(t)$ as $t \rightarrow 0$ implies that

$$\|\tilde{S}'_k(\cdot; z, \zeta) - \tilde{S}'_0(\cdot; z, \zeta)\|_{H^{-1/2}[0, 2\pi] \rightarrow H^{1/2}[0, 2\pi]} \leq c |\ln k| k^2 \|\zeta\|_{C^1[0, 2\pi]}. \quad (3.15)$$

Analogously, the parameterized mean value operator \tilde{M} is given by

$$(\tilde{M}\varphi)(t) = \frac{\int_0^{2\pi} \varphi(\tau) d\tau}{\int_0^{2\pi} |z'(\tau)| d\tau}, \quad t \in [0, 2\pi],$$

with Fréchet derivative

$$\tilde{M}'(\varphi; z, \zeta)(t) = - \int_0^{2\pi} \frac{z'(\tau) \cdot \zeta'(\tau)}{|z'(\tau)|} d\tau \frac{\int_0^{2\pi} \varphi(\tau) d\tau}{\left[\int_0^{2\pi} |z'(\tau)| d\tau \right]^2}, \quad t \in [0, 2\pi].$$

From this we conclude that for $\kappa = 0$ and $\kappa = k$ the corresponding parameterized operators \tilde{L}_κ are Fréchet differentiable with an estimate

$$\|\tilde{L}'_k(\cdot; z, \zeta) - \tilde{L}'_0(\cdot; z, \zeta)\|_{H^{-1/2}[0, 2\pi] \rightarrow H^{1/2}[0, 2\pi]} \leq c |\ln k| k^2 \|\zeta\|_{C^1[0, 2\pi]}. \quad (3.16)$$

Since \tilde{L}_κ has a bounded inverse and is Fréchet differentiable the inverse \tilde{L}_κ^{-1} and consequently the solution φ_κ of the parametrized form of (3.8) is also Fréchet differentiable. Differentiating (3.8) we obtain

$$\tilde{L}_\kappa \varphi'_\kappa(z, \zeta) = -\tilde{L}_\kappa \varphi_\kappa(z, \zeta) - \text{grad } u_{i, \kappa} \circ z \cdot \zeta \quad (3.17)$$

as integral equation for the derivative $\varphi'_k(z, \zeta)$. From this, putting (3.11), (3.12) and (3.16) together, with the aid of the Neumann series and the triangle inequality we obtain that

$$\|\varphi'_k(z, \zeta) - \varphi'_0(z, \zeta)\|_{H^{-1/2}[0, 2\pi]} \leq c \left(|\ln k| k^2 \|u_{i,0}\|_{H^{3/2}(\Gamma)} + \|u_{i,k} - u_{i,0}\|_{H^{3/2}(\Gamma)} \right). \quad (3.18)$$

The occurrence of the $H^{3/2}$ norm in (3.18) is due to the derivative of $u_{i,\kappa}$ in the integral equation (3.17).

For the Fréchet derivatives of the restriction of the parameterized potential operator $\tilde{\mathcal{L}}_\kappa$ onto Γ_1 as given by

$$\tilde{\mathcal{L}}_\kappa(|z'| \chi \circ z) = \mathcal{L}_\kappa(\chi)(x), \quad x \in \Gamma_1,$$

for all $\chi \in H^{-1/2}(\Gamma_0)$ and the corresponding normal derivative on Γ_1 we refrain from repeating ourselves and just note that their norms also satisfy an order $|\ln k| k^2$ estimate. Hence, differentiating $\tilde{\mathcal{L}}_k \varphi_k|_{\Gamma_1} - \tilde{\mathcal{L}}_0 \varphi_0|_{\Gamma_1}$ and the corresponding difference for the normal derivative on Γ_1 and estimating with the aid of the triangle inequality we finally arrive at

$$\|(F'_k(\Gamma) - F'_0(\Gamma))h\|_Y \leq c \left(|\ln k| k^2 \|u_{i,0}\|_{H^2(D_1)} + \|u_{i,k} - u_{i,0}\|_{H^2(D_1)} \right) \|h\|_{C^1(\Gamma)}$$

for all $\Gamma \in W_\eta$ and all $h \in C^1[0, 2\pi]$, that is,

$$\|F'_k(\Gamma) - F'_0(\Gamma)\|_{C^1(\Gamma) \rightarrow Y} \leq c \left(|\ln k| k^2 \|u_{i,0}\|_{H^2(D_1)} + \|u_{i,k} - u_{i,0}\|_{H^2(D_1)} \right) \quad (3.19)$$

for all $\Gamma \in W_\eta$.

For convenience, we assume that

$$\|u_{i,k} - u_{i,0}\|_{H^2(D_1)} \leq d |\ln k| k^2 \quad (3.20)$$

for some constant d and refer to this as **Assumption II**. Then the estimates (3.14) and (3.19) simplify into the form of the following lemma.

Lemma 3.1 *Under the Assumption II there exists $k_0 > 0$ such that for the operators F_k and F_0 we have that*

$$\|F_k(\Gamma) - F_0(\Gamma)\|_{H^{1/2}(\Gamma_1) \times H^{-1/2}(\Gamma_1)} \leq K |\ln k| k^2 \quad (3.21)$$

and

$$\|F'_k(\Gamma) - F'_0(\Gamma)\|_{C^1(\Gamma) \rightarrow H^{1/2}(\Gamma_1) \times H^{-1/2}(\Gamma_1)} \leq K |\ln k| k^2 \quad (3.22)$$

for all Γ in the neighborhood W_η of Γ_0 , all $0 < k \leq k_0$ and some constant K .

4 A convergence result

We are now ready to prove our main result.

Theorem 4.1 *Under the Assumptions I and II, with the constants occurring in (3.2) and in Lemmas 2.1 and 3.1 set*

$$\delta := \frac{\eta\sqrt{\alpha}}{2C}$$

and assume that

$$\|(f_H, g_H) - (f_L, g_L)\|_{H^{1/2}(\Gamma_1) \times H^{-1/2}(\Gamma_1)} \leq \frac{\delta}{2}, \quad (4.1)$$

$$\|(R_\alpha - R)(f_L, g_L)\|_{C^1[0, 2\pi]} \leq \frac{\eta}{2}, \quad (4.2)$$

$$CK|\ln k|k^2 < \sqrt{\alpha} \max\left(1, \frac{\eta}{4}\right). \quad (4.3)$$

Then the iteration operator J_α maps the ball $B[f_L, g_L; \delta] \subset H^{1/2}(\Gamma_1) \times H^{-1/2}(\Gamma_1)$ into itself and is a contraction, that is, the iteration scheme (1.17) with R replaced by R_α converges.

Proof. We abbreviate $B_\delta := B[f_L, g_L; \delta]$ and set $Z := C^2[0, 2\pi]$. For each $(f, g) \in B_\delta$, using (2.7), (4.2) and the definition of δ , we can estimate

$$\|R_\alpha(f, g) - R(f_L, g_L)\|_Z \leq \|R_\alpha[(f, g) - f_L, g_L]\|_Z + \|(R_\alpha - R)(f_L, g_L)\|_Z \leq \eta,$$

that is, in view of $R(f_L, g_L) = \Gamma_0$ the curve $R_\alpha(f, g)$ belongs to W_η . Hence, we can use (3.21), (4.1), (4.3) and the definition of δ to obtain

$$\|J_\alpha(f, g) - (f_L, g_L)\|_Y \leq \|(f_H, g_H) - (f_L, g_L)\|_Y + \|F_k(R_\alpha(f, g)) - F_0(R_\alpha(f, g))\|_Y \leq \delta$$

for all $(f, g) \in B_\delta$, that is, J_α maps B_δ into itself.

Again using $R_\alpha(f, g) \in W_\eta$ for all $(f, g) \in B_\delta$, with the aid of the mean value theorem and the inequalities (2.7) and (3.22) we can estimate

$$\begin{aligned} \|J_\alpha(f_1, g_1) - J_\alpha(f_2, g_2)\|_Y &\leq \sup_{\Lambda \in W_\eta} \|F'_k(\Gamma) - F'_0(\Gamma)\|_{Z \rightarrow Y} \|R_\alpha(f_1, g_1) - R_\alpha(f_2, g_2)\|_Z \\ &\leq \frac{KC|\ln k|k^2}{\sqrt{\alpha}} \|(f_1, g_1) - (f_2, g_2)\|_Y \end{aligned}$$

for all $(f_1, g_1), (f_1, g_1) \in B_\delta$, that is, in view of assumption (4.3) the operator J_α is a contraction. \square

Clearly, the limit (f_L^α, g_L^α) of the successive approximations

$$(f_{n+1}, g_{n+1}) := (f_H, g_H) + F_0(R_\alpha(f_n, g_n)) - F_k(R_\alpha(f_n, g_n)), \quad n = 0, 1, \dots,$$

starting with the initial guess $(f_0, g_0) = (f_H, g_H)$ satisfies

$$(f_L^\alpha, g_L^\alpha) = (f_H, g_H) + F_0(R_\alpha(f_L^\alpha, g_L^\alpha)) - F_k(R_\alpha(f_L^\alpha, g_L^\alpha)).$$

Subtracting from this the identity (1.16) yields

$$(f_L^\alpha, g_L^\alpha) - (f_L, g_L) = (F_0 - F_k)(R_\alpha(f_L^\alpha, g_L^\alpha)) - (F_0 - F_k)(R(f_L, g_L)).$$

Using the mean value theorem and (3.22) as in the above proof we can estimate

$$\|(f_L^\alpha, g_L^\alpha) - (f_L, g_L)\|_Y \leq K |\ln k| k^2 \|R_\alpha(f_L^\alpha, g_L^\alpha) - R(f_L, g_L)\|_Z.$$

From this with the aid of the triangle inequality and (2.7) and (4.2) we obtain

$$\|(f_L^\alpha, g_L^\alpha) - (f_L, g_L)\|_Y \leq \frac{KC |\ln k| k^2}{\sqrt{\alpha}} \|(f_L^\alpha, g_L^\alpha) - (f_L, g_L)\|_Y + \frac{1}{2} K \eta |\ln k| k^2.$$

In view of (4.3) this finally implies that

$$\|(f_L^\alpha, g_L^\alpha) - (f_L, g_L)\|_{H^{1/2}(\Gamma_1) \times H^{-1/2}(\Gamma_1)} \leq L |\ln k| k^2$$

for some constant L . From this, for the reconstructed curves, via the triangle inequality and (2.7) we obtain the estimate

$$\|R_\alpha(f_L^\alpha, g_L^\alpha) - \Gamma_0\|_{C^1[0, 2\pi]} \leq \frac{LC |\ln k| k^2}{\sqrt{\alpha}} + \|R_\alpha(f_L, g_L) - R(f_L, g_L)\|_{C^1[0, 2\pi]}.$$

with the right side tending to zero if k and α go to zero such that $|\ln k| K^2 / \sqrt{\alpha}$ tends to zero.

5 Numerical algorithm and results

5.1 Numerical implementation

In the above iterative procedure, we need the solution of the Cauchy problem for the construction of the interior boundary Γ_0 from the boundary function φ . To this end we expand $\gamma \circ \varphi$ in a Fourier series

$$(\gamma \circ \varphi)(t) = \sum_{n=-\infty}^{\infty} a_n e^{int}, \quad t \in [0, 2\pi],$$

and obtain Ψ by the Laurent series $\Psi(z) = \sum_{n=-\infty}^{\infty} a_n z^n$. Then, $t \mapsto \Psi(\rho e^{it})$, $t \in [0, 2\pi)$, gives a parametrization of Γ_0 . In order to numerically cope with the instability of this parametrization with respect to errors in the Fourier coefficients a_n for $n < 0$ we incorporate a regularization of Tikhonov type and shall also play with the truncation level of the series during iterations. The regularized parametrization will always be of the form

$$L_{\rho, \alpha, N}(t) := \sum_{n=0}^N a_n \rho^n e^{int} + \sum_{n=1}^N a_{-n} \frac{\rho^n}{\alpha_n + \rho^{2n}} e^{-int} \quad (5.4)$$

where $\alpha = (\alpha_1, \dots, \alpha_N)$ serves as a regularization parameter. Suggested by the algorithm described above, we implemented the following algorithm.

1. Initiate the iteration procedure with $(f, g) = (f_H, g_H)$ and $\varphi(t) = t$, $t \in [0, 2\pi]$, then find the integer $m_0 = m$ for which

$$\rho_0 = \left[\frac{b_m(\varphi; g) - |m| a_m(\varphi; f)}{b_m(\varphi; g) + |m| a_m(\varphi; f)} \right]^{\frac{1}{2|m|}}$$

has the closest value to a given threshold (we choose it equal to 0.5).

2. Initiate the number of Fourier coefficients by $N = N_{min} = 1$ and put $\alpha_N = \alpha_{min}$.
3. At step $n + 1$, start iterations for fixed (f, g) :
 - Update φ by solving the differential equation (1.5).
 - Update ρ using (1.10) with $m = m_0$.
 - Update $\Gamma_0 = R(f, g)$ using (5.4). If Γ_0 does not lie inside Γ_1 or Γ_0 has crossing points (see comments below), then decrease the number of Fourier coefficients $N = \max(N - 1, N_{min})$ and increase the regularization parameter $\alpha_N = 2\alpha_N$.
 - If $\|L_{\rho_{n+1}, \alpha, N} - L_{\rho_n, \alpha, N}\| \leq \delta \|L_{\rho_n, \alpha, N}\|$ then exit the current loop.
4. If $\|\varphi_{n+1} - \varphi_n\| \leq \delta \epsilon \|\varphi_n\|$ or $N = N_{max}$ then stop the iterations.
5. Increase N by one and set $\alpha_{N+1} = \alpha_N$.
6. Update (f, g) using (1.17).

Note that our algorithm gives more power to the regularization by Fourier truncation than to the Tikhonov regularization. This was suggested by numerical experiments since, for instance, the use of uniform regularization coefficients would decrease the accuracy of the final reconstruction. The algorithm contains some parameters: δ , ϵ , N_{max} , α_{min} , that have to be tuned. In our experiments, we took $\delta = 1\%$ and ϵ to be equal to the noise level. The choice of the other two parameters is less important and would only have effect on the number of iterations. In our experiments we took $\alpha_{min} = 0.001$ and $N_{max} = 10$.

Another issue with the algorithm was how to ensure that Γ_0 has no crossing points. We were not able to come up with a simple criterion that allows us to check this item. However, by requiring that the increment in the length of Γ_0 should be smaller than the increment in the parametrization norm we observed that the obtained parameterizations remain injective during iterations.

5.2 Numerical results

We choose D_1 to be the unit disk in all subsequent experiments. The data (f_H, g_H) used to solve the inverse problem are synthetically produced by numerical computation of the solution to the forward problem. Our forward solver is based on a boundary integral equation formulation of the problem and the use of a Nyström method with weighted trigonometric interpolation quadratures on an equidistant mesh, as explained in [2, Chapter 3]. The Cauchy data correspond with an incident field of the form

$$u_{i,k}(x) = \frac{2}{k} J_1(kr) e^{i\theta}$$

where (r, θ) denotes the polar coordinates of x . The associated incident field for the Laplace problem is

$$u_{i,0}(x) = x.$$

The Helmholtz Cauchy data is corrupted with 1% point wise random noise. We note that this incident field $u_{i,k}$ can be generated from plane incident waves using the Jacobi-Anger expansion,

$$J_1(kr) e^{i\theta} = \frac{-i}{2\pi} \int_0^{2\pi} e^{ikx \cdot d(\theta_0)} e^{i\theta_0} d\theta_0$$

with $d(\theta_0) := (\cos \theta_0, \sin \theta_0)$.

In the following examples we illustrate the satisfactory performance of the algorithm, even for moderate values of the frequency. We choose $k = 1.5$ which corresponds to a wavelength $\lambda = 4.2$, i.e., roughly 4 to 5 times the diameter of the

sought obstacles. We observed that for this range, the algorithm is always converging, as demonstrated by Figures 5.1–5.3. These figures correspond to obstacles Γ_0 with increasing non convexity and are parametrized by

$$z(t) = (0.2 + 0.4 \cos t + q \cos 2t, 0.4 \sin t), \quad 0 \leq t \leq 2\pi, \quad (5.5)$$

with increasing values $q = 0.1, 0.2, 0.3$ of the parameter q .

In all the figures the upper left shows the iterations of the reconstructed geometry and the upper right shows the final reconstruction (with the exact curve in dashed red). The bottom plots show the Cauchy data (f_n, g_n) during the iteration (the dashed red lines correspond to the Helmholtz data (f_H, g_H)). The relative amplitude of added random noise is 1% in all examples.

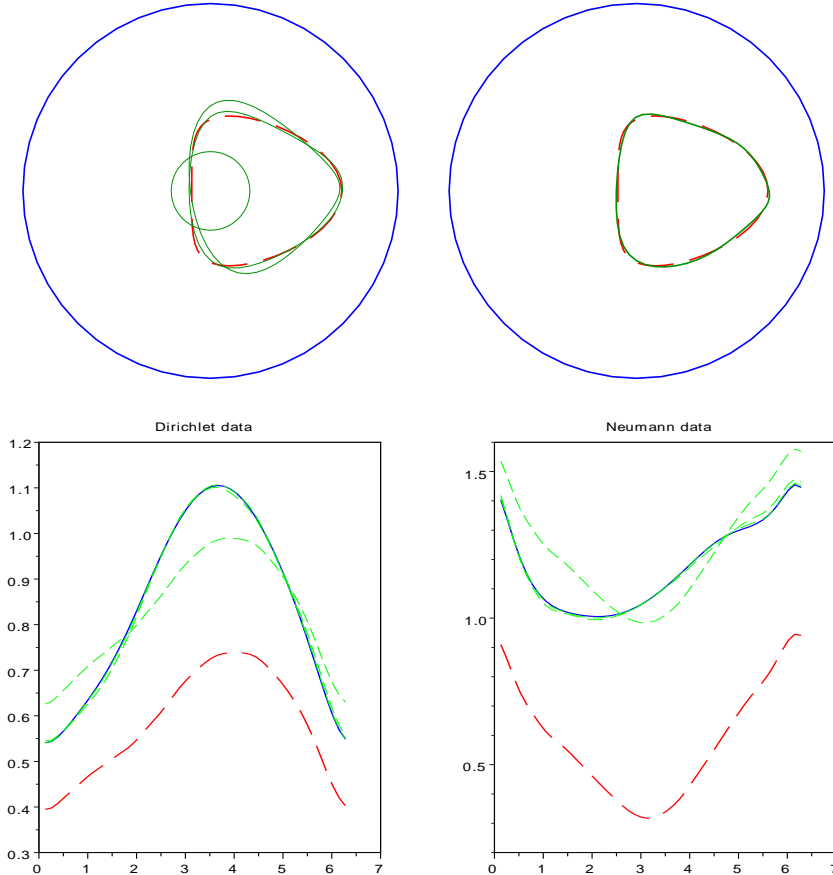


Figure 5.1: Frequency $k = 1.5$ and exact geometry (5.5) with $q = 0.1$.

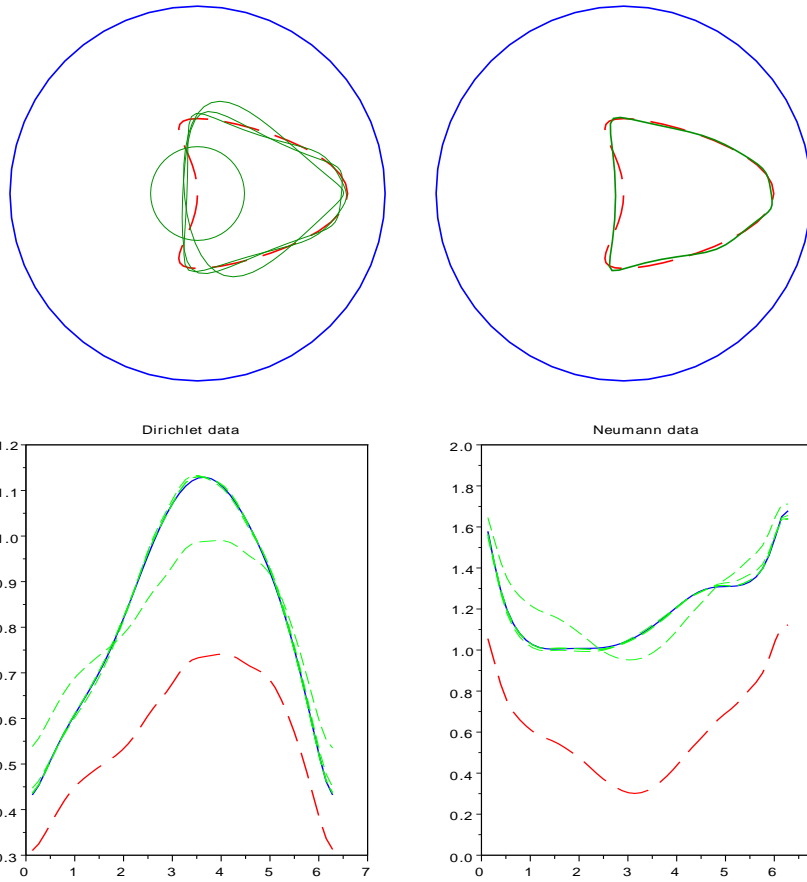


Figure 5.2: Frequency $k = 1.5$ and exact geometry (5.5) with $q = 0.2$.

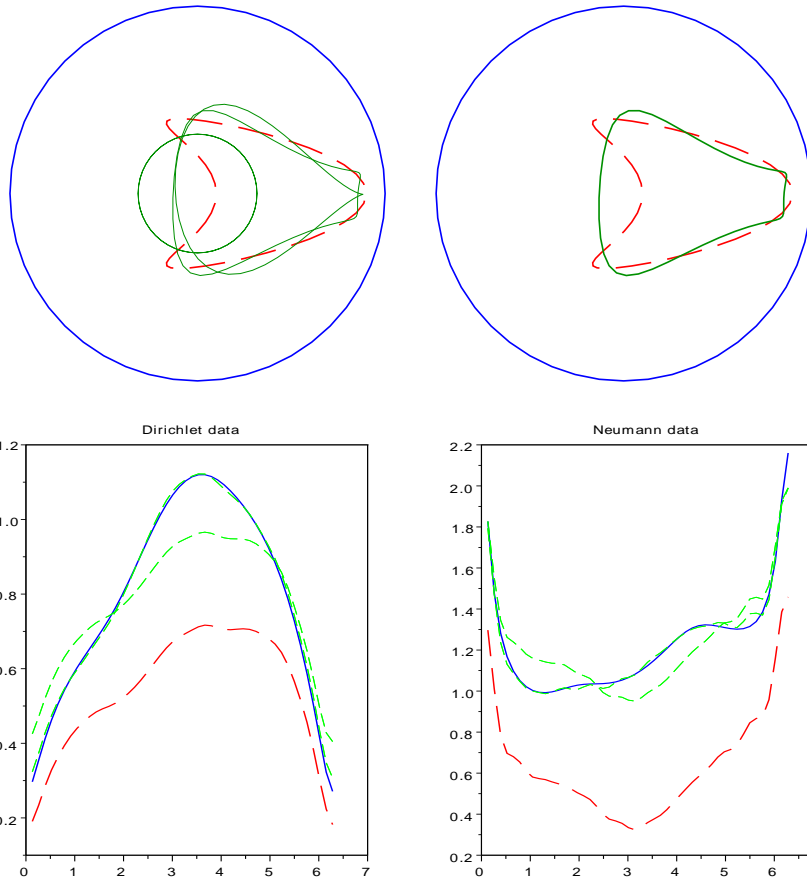


Figure 5.3: Frequency $k = 1.5$ and exact geometry (5.5) with $q = 0.3$.

For the frequency $k = 1.5$ we observe that the sequence (f_n, g_n) converges to (f_L, g_L) after a few iterations. Therefore the difference in the accuracy of the reconstruction of the geometry is mainly due to the conformal mapping algorithm and not to the use of data coming from the Helmholtz equation. Indeed better reconstructions are obtained for the convex obstacle, where only a few Fourier coefficients are necessary to obtain a good approximation of the shape.

In the next series of experiments illustrated in Figures 5.4-5.6 we maintained the same settings as for Figures 5.1-5.3 but increased the frequency to $k = 2$. As one observes, more iterations are needed for (f_n, g_n) to converge to (f_L, g_L) . Moreover, the accuracy deteriorates as the non convexity increases. In the convex case we obtain almost the same accuracy of reconstruction as for $k = 1.5$.

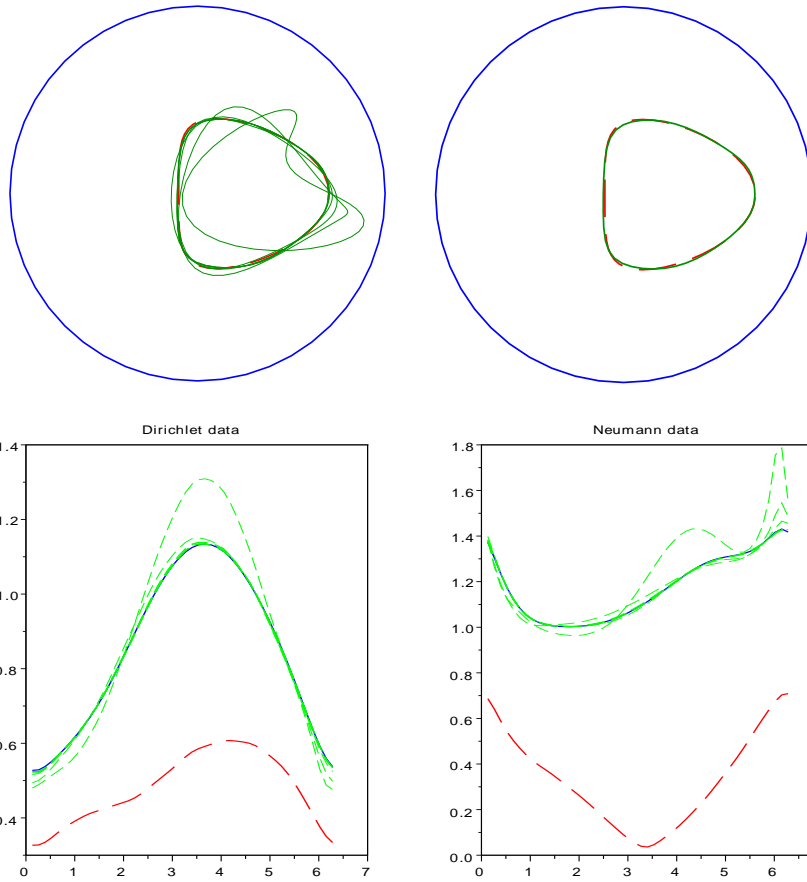


Figure 5.4: Frequency $k = 2$ and exact geometry (5.5) with $q = 0.1$.

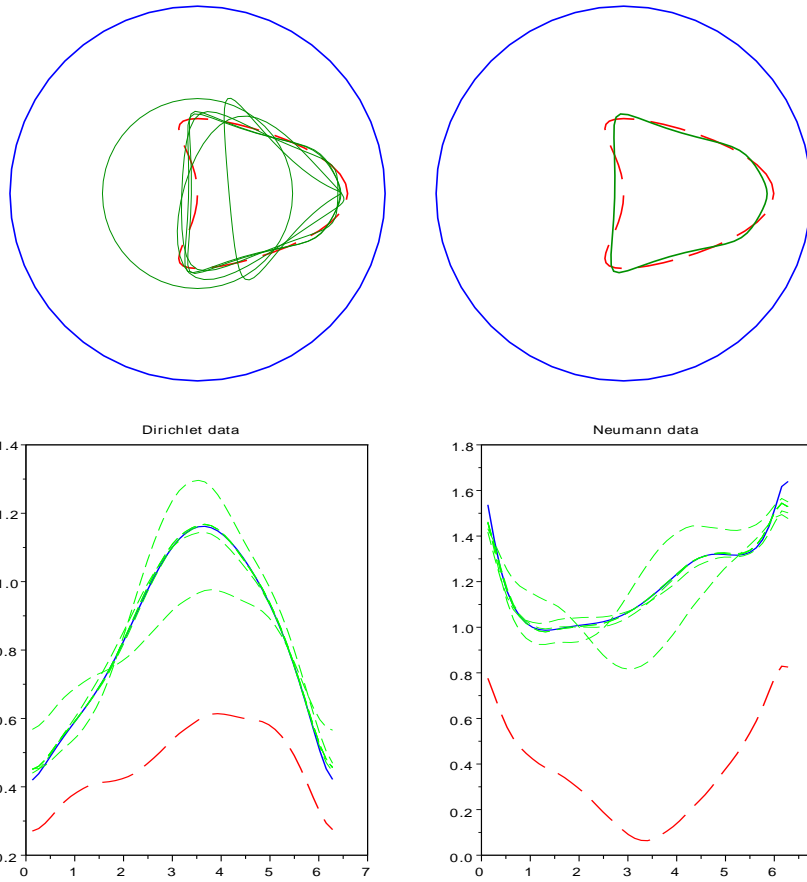


Figure 5.5: Frequency $k = 2$ and exact geometry (5.5) with $q = 0.2$.

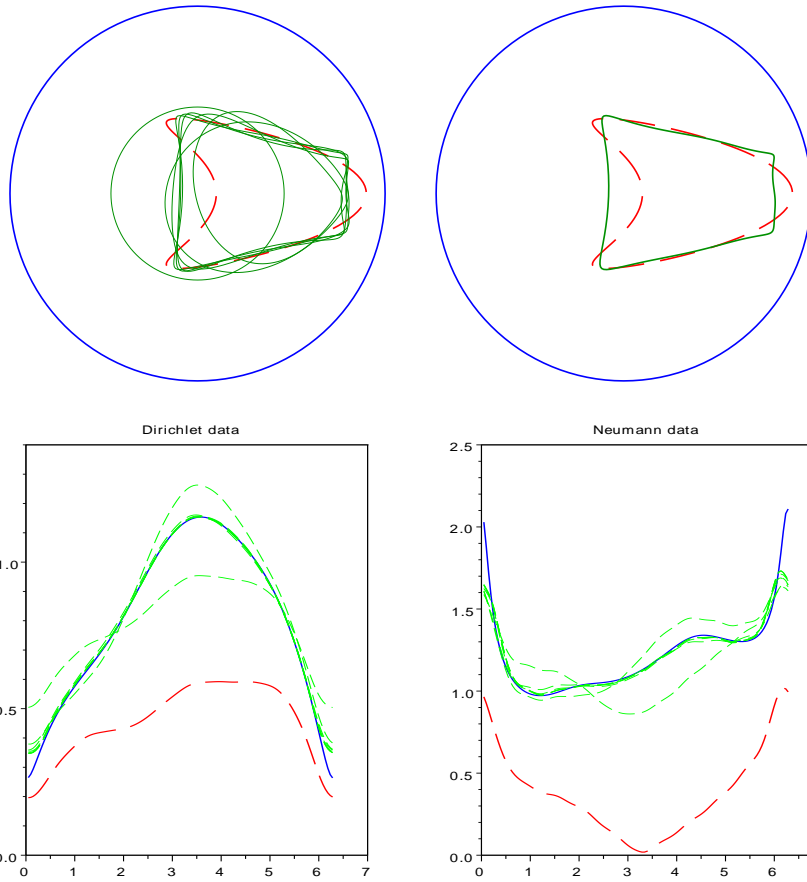


Figure 5.6: Frequency $k = 2$ and exact geometry (5.5) with $q = 0.3$.

Acknowledgement

Part of this research was carried out while R.K. was visiting INRIA Saclay Ile de France and Ecole Polytechnique, Palaiseau. The hospitality and the support are gratefully acknowledged.

References

- [1] Akduman, I. and Kress, R.: Electrostatic imaging via conformal mapping. *Inverse Problems* **18**, 1659–1672 (2002).
- [2] Colton, D. and Kress, R.: *Inverse Acoustic and Electromagnetic Scattering Theory*, 2nd. ed. Springer, Berlin, 1998.

- [3] Colton, D. and Kress, R.: Inverse scattering. In: *Handbook of Mathematical Methods in Imaging*, Scherzer, ed., Springer, Berlin, 2011, pp. 551–598.
- [4] Dassios, G. and Kleinman, R.: *Low Frequency Scattering*. Clarendon Press, Oxford, 2000.
- [5] Haddar, H. and Kress, R.: Conformal mappings and inverse boundary value problems. *Inverse Problems* **21**, 935–953 (2005).
- [6] Haddar, H. and Kress, R.: Conformal mapping and an inverse impedance boundary value problem. *Jour. on Inverse and Ill-Posed Problems* **14**, 785–804 (2006).
- [7] Haddar, H. and Kress, R.: Conformal mapping and impedance tomography. *Inverse Problems* **26**, 074002 (2010).
- [8] Kress, R.: On the low wave number asymptotics for the two-dimensional exterior Dirichlet problem for the reduced wave equation. *Math. Meth. in the Appl. Sci.* **9**, 335–341 (1987).
- [9] Kress, R.: On the low wave number behavior of two-dimensional scattering problems for an open arc. *Zeit. für Analysis und Anwend.* **18**, 297–305 (1999).
- [10] Kress, R.: *Linear integral equations*, 2nd ed. Springer, New York, 1999.
- [11] Kress, R.: Inverse Dirichlet problem and conformal mapping. *Mathematics and Computers in Simulation* **66**, 255–265 (2004).
- [12] Kress, R.: Inverse problems and conformal mapping. *Complex Variables and Elliptic Equations* **57**, 301–316 (2012).
- [13] Kress, R. and Rundell, W.: Reconstruction of extended sources for the Helmholtz equation. Submitted.
- [14] Potthast, R.: Fréchet differentiability of boundary integral operators in inverse acoustic scattering. *Inverse Problems* **10**, 431–447 (1994).
- [15] Wegmann, R.: Methods for numerical conformal mapping. In *Handbook of Complex Analysis: Geometric Function Theory, Vol 2*, Kühnau, ed., North Holland, Amsterdam, 2006, pp. 351–477.
- [16] Werner, P.: Low frequency asymptotics for the reduced wave equation in two-dimensional exterior spaces. *Math. Meth. in the Appl. Sci.* **8**, 134–156 (1986).